



Research article

Metabolomic profile of medicinal plants with anti-RVFV activity



Garland Kgosi More ^{a,*}, Jacques Vervoort ^{b,c}, Paul Anton Steenkamp ^d, Gerhard Prinsloo ^b

^a College of Agriculture and Environmental Sciences, University of South Africa, Johannesburg, South Africa

^b Department of Agriculture and Animal Health, University of South Africa, Johannesburg, South Africa

^c Laboratory of Biochemistry, Wageningen University & Research, Wageningen, the Netherlands

^d Department of Biochemistry, Research Centre for Plant Metabolomics, University of Johannesburg, Johannesburg, South Africa

ARTICLE INFO

Keywords:

¹H-NMR-Metabolomics

UHPLC-qTOF-MS

Medicinal plants

Anti-viral

Rift valley fever virus

ABSTRACT

Twenty medicinal plants with previously established anti-viral activity against a wild-type RVFV were further investigated using bio-chemometric and analytical techniques. The aim being to identify compounds common in plants with anti-RVFV activity, potentially being the major contributors to the anti-viral effect. Proton nuclear magnetic resonance (¹H NMR) spectroscopy coupled with multivariate data analysis (MVDA) was applied to characterize metabolite profiles of twenty antiviral medicinal plants. Discrimination and prediction of metabolome data of active anti-RVFV from the less-active samples was assessed using the multivariate statistical models by constructing a robust principal component analysis (PCA) and orthogonal partial least squares discriminant analysis (OPLS-DA) regression model. Annotation of metabolites in the samples with higher activity were performed by Chemox software and the compounds confirmed using Ultra-High-Performance Liquid Chromatography-Quadrupole Time-of-Flight Mass Spectrometry (UHPLC-qTOF-MS). Both the PCA and OPLS-DA score plots showed clustering of samples; however, the OPLS-DA plot indicated a clear separation among active and less-active samples. Metabolic biomarkers were screened by *p*-value < 0.05 and variable importance in the projection (VIP) value >1 and S-plot. Among active samples, the most prominent metabolites putatively identified by NMR include trigonelline, vanillic acid, fumarate, chlorogenic acid, ferulate, and formate. The presence of the compounds were confirmed by UHPLC-qTOF-MS, and two hydroxylated fatty acids were additionally detected indicated by peaks at *m/z* 293.2116 and *m/z* 295.2274 13S-Hydroxy-9Z,11E,15Z-octadecatrienoic acid and 13-Hydroxy-9Z,11E-octadecadienoic acid were annotated for the first time in all the antiviral active samples and are considered potential metabolites responsible for the antiviral activity. The study provides a metabolomic profile of anti-RVFV plant extracts and report for the first time the presence of hydroxylated fatty acids 13S-Hydroxy-9Z,11E,15Z-octadecatrienoic acid and 13-Hydroxy-9Z,11E-octadecadienoic acid, present in all the tested medicinal plants with high anti-RVFV activity and is a potential target for the future development of antiviral therapeutic agents.

1. Introduction

Medicinal plants are a rich source of secondary metabolites that have shown to contain potential leads for drugs in the field of therapeutic drug discovery and development. There are more than 100 new therapeutic drugs from natural products in clinical development as potential anti-cancer, antidiabetes, and antimicrobial agents (Woalder 2015). The discovery of new drug leads from natural products is a lengthy and incremental ongoing process that has recently employed technological practices such as “omics” methodologies to accelerate the discovery and development of new therapeutic agents (Mohana et al., 2018; Quansah

and Karikari 2016). As part of the omics technologies; metabolomics is a technique that focuses on a high-throughput identification and quantification of metabolites in a biological organism. It is capable of identifying and discriminating metabolites that are of significant importance within the metabolome (Choi and Verpoorte 2014). The advent of metabolomics technique has aroused interests in non-targeted metabolomic mappings such as quality control of plant products, diagnostics, agriculture and environmental monitoring (Chen et al., 2014; Emwas et al., 2019). These techniques have shown to be economically sustainable and also proven efficient in natural product discovery (Mohana et al., 2018). Earlier studies reported the use of metabolomic techniques

* Corresponding author.

E-mail address: moregk@unisa.ac.za (G.K. More).

in various disease diagnosis including cancer, diabetes, human immunodeficiency virus (HIV), tuberculosis (TB) to mention a few, using blood, urine and faecal materials in assessing metabolite changes (Urvinder et al., 2020; Vrieling et al., 2019; Heyman et al., 2015; Prinsloo and Vervoort 2018). Among differential combinations of NMR and LC-MS platforms, Heyman et al. (2015) identified anti-human immunodeficiency virus (HIV) metabolites from South African *Helichrysum* species and this study lead to the identification of dicaffeoylquinic and tricaffeoylquinic acids in *Helichrysum populifolium*. Prinsloo and Vervoort (2018) identified anti-Herpes simplex virus (HSV) compounds from unrelated plants using NMR and LC-MS metabolomic analysis. Chlorogenic acids were identified as common compounds in plants that exhibited anti-HSV activity. In our previous study More et al. (2021), the antiviral activity of twenty medicinal plants against the Rift Valley Fever Virus (RVFV) was demonstrated. Eight out of twenty active plant extracts showed potency against the RVFV. This study aimed to conduct ^1H NMR metabolomic analysis coupled with multivariate data analysis and UHPLC-qTOF-MS to identify compounds contributing to the antiviral activity observed in our previous study.

2. Materials and methods

2.1. Sample preparation and NMR analysis

Twenty different plant species known for their anti-viral properties against various viruses were selected based on their ethnobotanical uses and *in-vitro* pharmacological antiviral activities obtained in scientific literature (Table 1). Active and less-active samples against RVFV were determined in a previous study (supplementary material figure 1) using the cytopathic effect (CPE) reduction method (More et al., 2021). The pulverized leaf samples (50 mg) of all the samples were extracted with 750 μL of methanol- d_4 ($\text{CH}_3\text{OH}-d_4$) and 750 μL of potassium dihydrogen phosphate (KH_2PO_4) buffer in deuterium water (D_2O) (pH 6.0) containing 0.01 % (w/w) trimethylsilanepropionic acid (TSP). The mixture was vortexed for 1 min, ultra-sonicated for 20 min and then centrifuged for 20 min (10,000 rpm). Samples were then filtered through a 0.22 μm syringe filter. Finally, filtrates (500 μL) were transferred to a 5 mm standard NMR tube (Norell, Sigma-Aldrich). All the proton NMR spectra were acquired using a 600 MHz NMR spectrometer (Varian Inc, CA, USA) applying consistent settings.

Human immune deficiency virus (HIV-1,2; RT- Reverse transcriptase, PR-protease, CB- cell-based assay, FRET-fluorescence resonance energy transfer), Herpes simplex virus type (HSV-1,2), African swine fever virus (ASFV), Newcastle disease virus (NDV), Canine distemper virus (CDV), canine parainfluenza virus-2 (CPIV-2), feline herpesvirus-1 (FHV-1), Poliovirus (PV-2), Cytomegalovirus (CMV), lumpy skin disease virus (LSDV), coxsackie B virus (COX B-1), Adenovirus 31 (AD-31), Foot and Mouth disease virus (FMDV), Hepatitis B Virus (HBV), Epstein-Barr virus (EBV).

2.2. Multivariate data analysis

Data analysis and processing were performed using MestReNova software (9.0.1, Mestrelab Research, Spain), correction of phasing and baseline, normalisation and peak alignment was done manually on the ^1H -NMR spectrum (supplementary material figure 2a–2t). All processed data were binned in 0.04 ppm bins, representing 0–10 ppm and converted to Excel CSV file format for pattern recognition multivariate data analysis. Transformed data was statistically analysed, all the imported data Pareto scaled in the soft independent modelling of class analogy (SIMCA) software (SIMCA, Version 15.0.2, Umetrics, Umeå, Sweden). Active and non-active samples were statistically discriminated using the principal component analysis (PCA) and orthogonal projections to latent structure discriminant analysis (OPLS-DA). Annotations of compounds

Table 1. Selected anti-viral plants, their family names, and antiviral activities.

Plant names	Family	Antiviral activities	References
<i>Sutherlandia frutescens</i>	Fabaceae	HIV1 RT, IN, RNase H	Bessong et al., (2005), 2006; Harnett et al., (2005)
<i>Prunus africana</i>	Rosaceae	CMV	Tolo et al., (2007)
<i>Carissa edulis</i>	Apocynaceae	HSV-1 CDV, CPIV, FHV, LSDV PV-2 CMV	Mukhtar et al. (2008); Tolo et al., (2006) Bagley (2018) Al-youssef and Hassan (2014) Tolo et al., (2007)
<i>Elaeodendron transvaalense</i>	Celastraceae	HIV-1, RT, CB, IN	Tshikalange et al., (2008); Bessong et al., (2005), 2006
<i>Terminalia sericea</i>	Combretaceae	HIV1 RT HIV-1 RNA-dependent-DNA polymerase (RDDP)	Tshikalange et al., (2008) Bessong et al., (2005)
<i>Crinum macowanii</i>	Amaryllidaceae	HIV-1 RT, PR	Klos et al., (2009)
<i>Ziziphus mucronata</i>	Rhamnaceae	HIV-1 RT, RNase H	Bessong et al., (2005)
<i>Helichrysum aureonitens</i>	Asteraceae	HSV-1, reovirus	Meyer et al., (1997)
<i>Euclea natalensis</i>	Ebenaceae	HSV-1	Lall et al., (2017)
<i>Senna petersiana</i>	Fabaceae	HIV1-RT	Tshikalange et al., (2008)
<i>Adansonia digitata</i>	Malvaceae	HSV-1 NDV HSV-1; ASFV HIV1 RT, HIV-FRET, PR	Rathore et al., (2007) Sulaiman et al., (2011) Silva et al., (1997) Sharma and Rangari (2016)
<i>Lobostemon fruticosus</i>	Boraginaceae	HIV-1	Lunat (2011)
<i>Peltophorum africanum</i>	Fabaceae	HIV1-RT	Theo et al., (2009); El-Toumy et al., (2018)
<i>Aloe ferox</i>	Asphodelaceae	HSV-1	Chen et al., (2012); Wintola et al., (2010)
<i>Heteropyxis natalensis</i>	Heteropyxidaceae	HIV-1 RT	Hurinanthan (2013)
<i>Artemisia afra</i>	Asteraceae	HIV-1/2	Liu et al., (2009); Asres et al., (2001)
<i>Ricinus communis</i>	Euphorbiaceae	HIV1- RT, RNase H, IN	Bessong et al., (2005), 2006
<i>Elephantorrhiza elephantina</i>	Fabaceae	HIV-RT	Sigidi et al., (2017)
<i>Elaeodendron croceum</i>	Celastraceae	HIV	Prinsloo et al., (2010)
<i>Moringa oleifera</i>	Moringaceae	HSV1 HIV-1 RT FMDV HBV, EBV	Hafidh et al., (2009); Lipipun et al., (2003) Karimi et al., (2015) Younus et al., (2015) Feustel et al., (2017) Terasaki et al., (2011)

were performed using the Chemomx software (NMR suite, version 8.3) and published NMR data.

2.3. Sample preparation and Ultra-High-Performance Liquid Chromatography-Quadrupole Time-of-Flight Mass Spectrometry (UHPLC-qTOF-MS) analysis

Pulverized leaves (5 mg) were extracted with 1.5 ml of 80% methanol (LC-grade and ultrapure LC-grade water), homogenized, ultrasonicated

for 5 min, and the homogenates were centrifuged for 15 min. The extract of each sample was then filtered using 0.22- μm nylon syringe filters and the filtrates were concentrated by evaporation to dryness. The dried extract was resuspended with 300 μL of 50 % methanol and pipetted into 2 mL HPLC glass vials. Aliquots of extracts were prepared in triplicates and stored at -20 °C before analysis.

The chromatographic separation and mass spectrometry detection were performed following a slightly modified method on a Waters Classic UHPLC coupled in tandem to a Waters SYNAPT G1 HDMS mass spectrometer. An HSS T3 C18 column (150 mm × 2.1 mm, 1.8 μM), thermostatted at 60 °C was used to obtain the separation of metabolites. Elution solvents (Eluent A: 10 mM formic acid and acetonitrile (Eluent B) containing 10 mM formic acid were used at a flow rate of 0.4 mL/min. The initial mobile consisted of 98 % A and kept for 1 min. The gradient applied started from 98 % A and changed to 5% A at 25 min. These conditions were maintained for 2 min and thereafter returned to initial mobile phase conditions. To avoid variations in data, samples were run in triplicates and solvent blanks were included in the run.

2.4. Quadrupole time-of-Flight Mass Spectrometry (q-TOF-MS) analyses

The Waters SYNAPT G1 Q-TOF system was used in V-optics mode to obtain high resolution mass spectra. Electrospray analysis was done in positive and negative ionisation mode to enable detection of phenolic compounds and other ESI-compatible compounds. Conditions were set as follows: typical mass accuracies between 1 and 5 mDa were obtained by lock mass calibrant using leucine enkephalin (50 pg/mL) as reference. The spectrometer was operated in both ESI positive and negative modes with a capillary voltage of 2.5 kV with the sampling cone at 30 V and the extraction cone at 4.0 V. The source temperature was 120 °C and the desolvation temperature was set at 450 °C. Nitrogen gas was used as the nebulisation gas at a flow rate of 550 L h⁻¹ and cone gas was added at 50 L h⁻¹. MassLynx v4.1 (SCN 872) software was used to control the hyphenated system and to perform all data manipulation. MassFragment v.2.0.w.15 was used to evaluate all mass spectra in relation to proposed structures.

3. Results

3.1. ¹H-NMR metabolomic analysis

The analyses of the ¹H-NMR spectroscopy data of plant metabolic profiles and performance of the multivariate data analyses to discriminate between active and non-active plant extracts were done using SIMCA software (Umetrics, Umeå, Sweden). The unsupervised pattern recognition analysis (PCA) was applied to give an overview of the dimension of the samples. The OPLS-DA, which is a supervised recognition analysis that allows the algorithm to expose discrimination between groups was applied to the data set. The distance to model X (DModX) was used to identify and remove outliers that fall outside the 95 % confidence region of the model. The variance of 95 % and coefficient $R^2 = 0.701$ and $Q^2 = 0.706$ values were used to validate the goodness and predictability of the model. Observation of the PCA score plot (Figure 1a) showed slight separation among samples, however, the hierarchical cluster analysis (HCA) dendrogram was developed to evaluate whether some groupings from the data can be generated. The HCA dendrogram grouped subjects with similar features into three clusters (Figure 1b, groupings: red, blue, and green), which suggested that the samples could be differentiated. The HCA analysis confirmed the separation of the samples into the two groups (Figure 1d), revealing underlying patterns of the data. For better separation, the OPLS-DA score plot was created, and it showed significant discrimination between the active (red circles) and less-active (blue circles) samples with an $R^2\text{X}$ value of 0.830 and a Q^2 value of 0.706 (Figure 1c). The HCA analysis confirmed the separation of the samples into the two groups (Figure 1d).

The OPLS-DA model was further validated using multivariate statistical tools and analysed by assessing the predictivity, reliability, and its significance. Validation was performed using the permutation test ($n = 100$), to evaluate the classification performance. Permutation analysis was done to further validate the model and 100 permutation tests with an $R^2\text{X} = 0.851$ and $Q^2 = 0.561$ was observed (Figure 2a). The receiver operating characteristic (ROC) which calculates the area under the curve (AUC) was plotted and the cross-validated predictive residual was performed (CV-ANOVA, p -value < 0.05). The ROC (AUC) = 0.9980 with a p

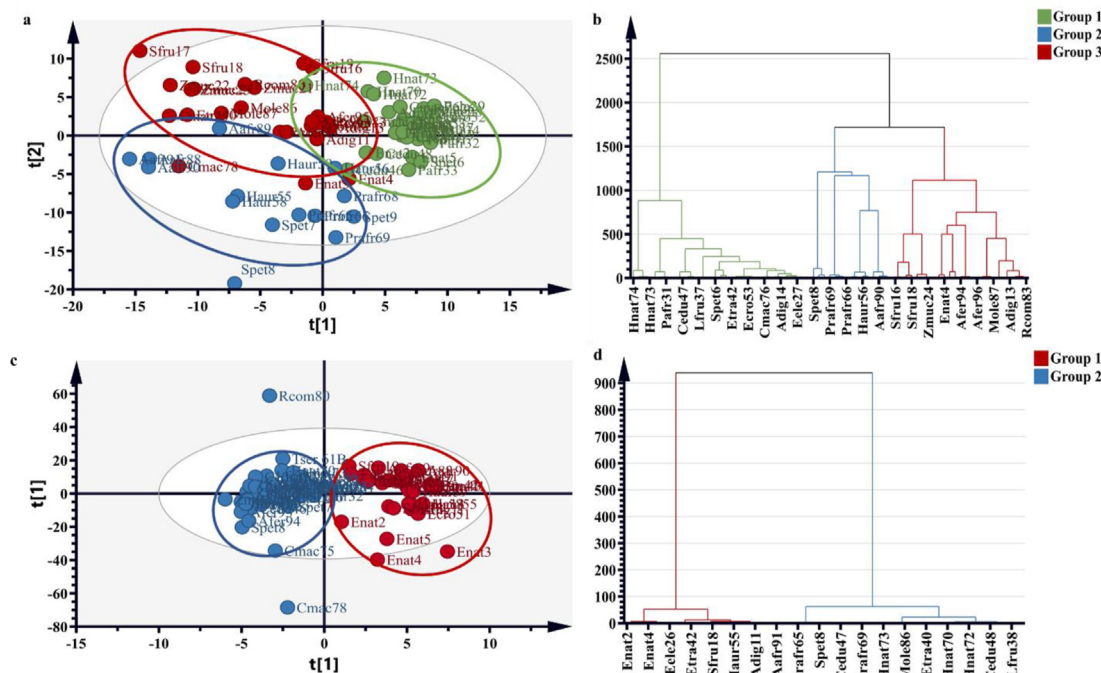


Figure 1. PCA (a) and OPLS-DA (c) score plots of 20 different aqueous methanol plant extracts with HCA dendograms derived from the PCA (b) and OPLS-DA (d) showing metabolic relativity of the samples. All plant samples were tested in replicated of five.

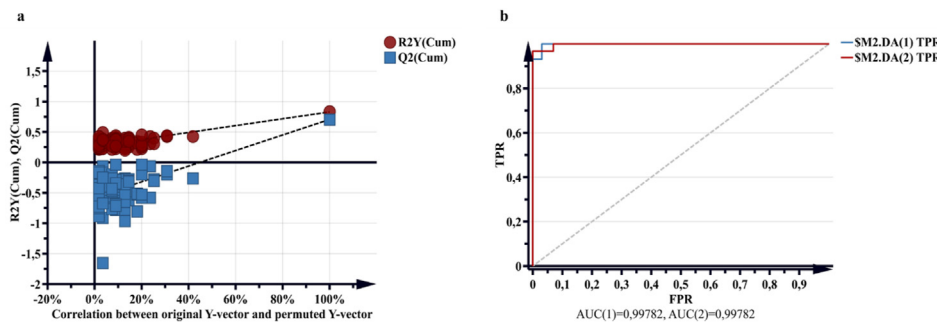


Figure 2. Statistical validation (a) of the OPLS-DA model by permutation testing ($n = 100$ permutations) and diagnostic performance through ROC ($AUC = 0.9980$) (b) analysis.

value $= 2.30 \times 10^{-12} \pm 2.08$ was obtained (Figure 2b). Overall, the statistical validation showed the reliability and predictability accuracy of the model.

Adopted to the supervised OPLS-DA results, the variable importance in the projection (VIP) values were predicted, which were arranged from the most significant variables from left to right (Figure 3a). Chemical shifts of the VIP scores >1 were considered significant contributors to the separation of samples. Discriminative variables were identified using the loading S-plot (Figure 3b) which showed bucket values of 2.24, 3.56, 3.68, 4.76, 4.72 and 4.80 ppm as major discriminants of the two groups. The loading S-plots also demonstrated that variables on the two extreme ends of the S-plot are discriminative with variables in group 1 (blue circle) of Figure 3b being the less-active group and the group 2 (red circle) being active. VIP scores and the S-plot helped to distinguish NMR regions to understand which variables were responsible for the separation and biological activity.

In addition, the contribution plot (Figure 4) revealed regions that are positively associated to the activity (0.92, 1.32, 1.44, 1.56, 1.60, 1.64, 1.68, 2.04, 2.12, 2.20, ppm bucketed values) in the aliphatic region, while the presence of some esters and carbonyl compounds were shown by bucket values 3.36, 3.68, 3.72, 3.76, 3.92, 3.96, 4.04, 4.24, 4.32, 4.40, 4.44, 4.48, 4.52, 4.56, 4.64, 4.68, 4.72, 4.76, 4.80, 4.84, 4.88, 5.28, 5.44, 5.48, 5.52, 5.64, 5.68, 5.88, 5.92 and 5.96 ppm in the sugar region. The presence of aromatic compounds was shown by the bucket values such as 6.0, 6.40, 6.48, 6.92, 7.64 and 7.68 ppm in the aromatic region. It is evident that the NMR spectral regions contributing to the activity of samples are mostly the aliphatic and sugar regions (positive bars). Regions 1.88–2.2 ppm (aliphatic) and 4.12–5.90 ppm (sugar) show prominent positively associated peaks, indicating metabolites responsible for the activity.

Chenomx software, PubChem, and published data were used to annotate metabolites by linking the important NMR spectral regions to metabolites responsible for the grouping of the anti-RVFV samples (supplementary material fig. 1). Proton NMR spectra of eight active plant samples were overlaid using MestReNova software and prominent NMR regions were noted which were matched with the peak profiles of potential metabolites in the active samples using Chenomx software

(Table 2). This analysis showed the prevalence of high concentrations of trigonelline, chlorogenate, formate and fumarate. The NMR spectra (Figure 5) showed prominent secondary metabolites present in anti-viral extracts namely chlorogenic acid, ferulic acid and vanillic acid. In the high-field region of the ^1H NMR spectra (0.8–4.5) of aqueous methanolic extracts, the most abundant peaks correspond to alanine, leucine, and acetic acid. Other compounds occurring in this region that are reported in the literature include valine, isoleucine, lactate, threonine, arginine, lysine, gamma-Aminobutyric acid (GABA), glutamic acid and proline (Lawal et al., 2017). The presence of chlorogenic acid and similar compounds such as 4,5-dicaffeoylquinic acid (Liu et al., 2009; Tabassum et al., 2016), and gallic acid (Dhanani et al. 2016) which are more prominent in the aromatic region were also observed.

3.2. UHPLC-qTOF-MS analysis results

The Ultra-High-Performance Liquid Chromatography-Quadrupole Time-of-Flight Mass Spectrometry (UHPLC-qTOF-MS) analysis was performed to assess metabolites in selected antiviral plants. Chromatograms obtained in the positive and negative ion modes were analysed with the MassLynx™ v4.1 SCN 872 software (Waters Corporation, Milford USA) which led to the tentative identification of 63 metabolites (Table 3) that are prominent in anti-RVFV samples. Chemical profiling of compounds was carried out by comparing the mass spectra, retention time (Rt), ion fragments with data from various databases including, NIST (National Institute of Standards and Technology) database, DNP (Dictionary of Natural Products: www.dnp.chemnetbase.com), MassBank (USA), mzCloud (Advanced Mass Spectral Database). In addition to the in house data analysis also MAGMa (www.emetabolomics.org) was used as well to check for the annotation of the measured masses and mass fragments using KEGG/HMDB/PubChem databases. Finally, the annotated compounds were compared to literature data. Characterization of metabolites from the antiviral samples showed that phenolic and flavonoids classes of compounds were more prominent in all samples. Chlorogenic acid-type metabolites were prominent compounds in *A. afra* and *H. aureonitens* extracts. The mass spectrum of *A. afra* and *H. aureonitens* extracts showed peaks at m/z 354.09508 and m/z 515.1195, which were esterified

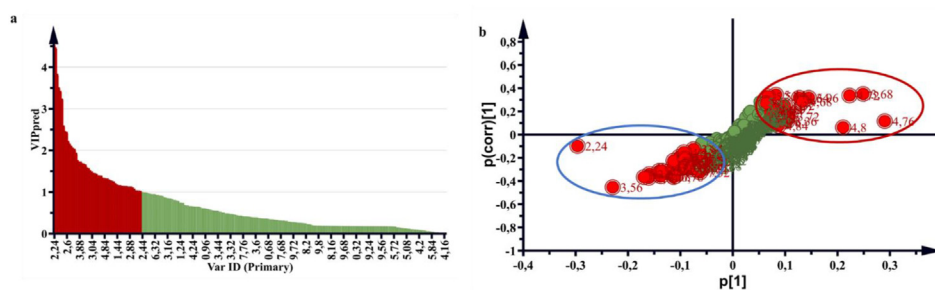


Figure 3. Identification of significant NMR regions contributing to the separation of samples in OPLS-DA by a VIP score plot annotated with chemical shift (ppm). Red coloured bars/dots representing metabolites with a VIP score greater than 1 which contribute significantly to the separation than green bars/dots which are metabolites with a VIP score less than 1. S-plot b with red circle indicating NMR regions being positively associated with the antiviral activity and blue circles representing NMR regions with less antiviral activity.

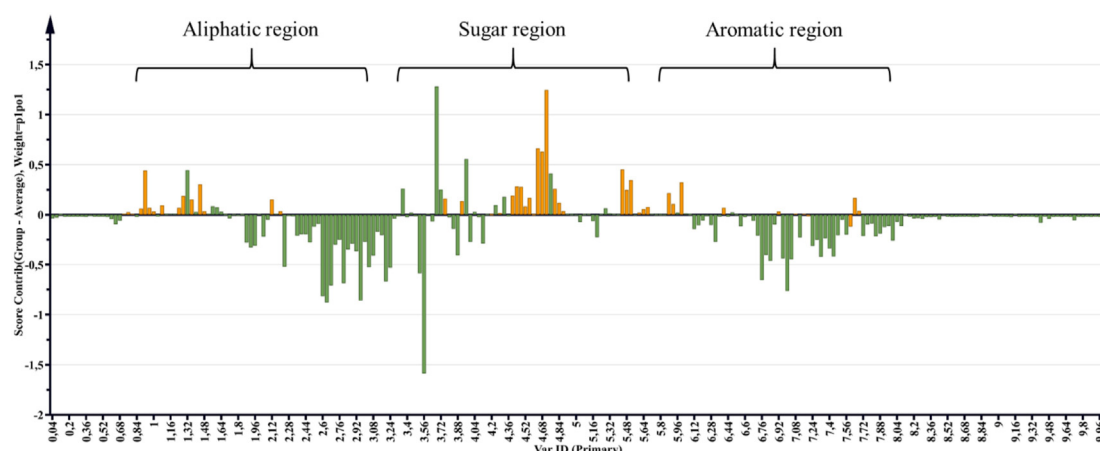


Figure 4. A contribution plot showing significant ^1H NMR spectral regions responsible for the separation of the active from the less-active samples. Positive scores are regions that are positively associated with activity and the negative scores are regions that are negatively associated with the activity. The contribution plot shows an increase in most metabolites in aliphatic and sugar, regions, which contributed to the separation of the samples.

Table 2. Chenomx assisted annotation of metabolites in anti-RVFV active samples. Presented are metabolites, major peaks chemical shift (ppm) and peak multiplicity (s = singlet; d = doublet; q = quartet; m = multiplet).

Annotated metabolite	Chemical shift (ppm)
Leucine	δ0.96 (d)
Acetate	δ1.98 (s)
Alanine	δ1.50 (d)
Citrate	δ2.50 (d)
Fumarate	δ6.50 (s)
Formate	δ8.47 (s)
Ferulic acid	δ6.38 (d)
Chlorogenic acid	δ6.30 (d)
Vanillate	δ7.44 (dd)
Trigonelline	δ9.15 (s)
Hydroxycaffeic acid	δ8.05 (d)

compounds indicating the presence of caffeoylquinic acids and dicaffeoylquinic acids such as 3-caffeoylelquinic acid, 4-caffeoylelquinic acid, 5-caffeoylelquinic acid, 4,5-dicaffeoylquinic acid, 3,5-dicaffeoylquinic acid and 3,4-dicaffeoylquinic acid. Vanillic acid and ferulic acid were observed at m/z 167.0325, and m/z 193.0488, respectively. The extracts also showed an ion peak at m/z 193.0488 and this peak was assigned to chlorogenic acid while quinic acid was detected at m/z 191.0546.

A flavonoid, kaempferol and flavonol glycoside, kaempferol 3-O-rutinoside were also annotated at m/z 285.0374 and m/z 593.1509, respectively. Other significant flavonols depicted in this analysis include quercetin and quercetin 3-rutinoside-7-glucoside shown by peaks at m/z 301.0305 and 771.1982, respectively. Observance of m/z 289.0716, 307.0763 and 289.0692 were assigned to flavan-3-ol type of chemical compound including catechin, galocatechin, epi-catechin famously known for their abundance among foods, fruits and green tea were present in *E. croceum*, *E. elephantina* and *A. digitata*. Of importance in this study is the putative identification of two hydroxylated fatty acid derivatives of linoleic acid at m/z 293.2116 and m/z 295.2274, annotated for the first time in all the anti-RVFV samples and are reported as 13S-Hydroxy-9Z,11E,15Z-octadecatrienoic acid and a similar compound 13-Hydroxy-9Z,11E-octadecadienoic acid. Trigonelline was present in *A. digitata*, *E. elephantina* and *S. frutescens* shown by a precursor ion at m/z 138.0555 with a product ions m/z 110.06; 94.06. Other annotated compounds unique to specific samples include the presence of terpenoids such natalenone in *E. natalensis*, elaeodendrol occurring *E. transvaalense*, digitoxigenin glucoside, elaeodendroside U in *E. croceum* and four

terpenoid saponins cycloartanol glycosides sutherlandioside A-D, and four flavonoids sutherlandin A-D present in *S. frutescens*.

4. Discussion

The eight promising anti-RVFV leaf aqueous-methanolic extracts were analysed using NMR spectroscopy to determine variations in polar metabolites and their correlation to the biological activity. The annotation of metabolites showed the presence of some important phytoconstituents like chlorogenic acid, ferulic acid, vanillic acid and trigonelline which were most prominent in the active extracts and previous studies reported the antiviral potency of these metabolites. These compounds as well as several other compounds were also detected by the UHPLC-qTOF-MS analysis.

Phenolic acids are strong antimicrobial and pro-oxidants which play a crucial role in several biological and pharmacological activities and they have antiviral potency (Naveed et al., 2018). Previous studies revealed the antiviral effects of chlorogenic acid against influenza A viruses on MDCK cells: A/PuertoRico/8/1934 (H1N1) and A/Beijing/32/92(H3N2) viruses with EC₅₀ values of 44.87 μM and 62.33 μM , respectively (Ding et al., 2017). Furthermore, chlorogenic acid, gallic acid and trigonelline showed strong inhibitory activity of parainfluenza (type-3) virus by inhibiting the CPE on Vero cells and these compounds exhibited the minimum inhibitory concentration (MIC) values of 0.4, 0.05 and 0.4 $\mu\text{g/mL}$, respectively (Özçelik et al., 2011). In a comprehensive review compiling the bioactive compounds of *Artemisia* species, chlorogenate type compounds such as chlorogenic acid, cryptochlorogenic acid, and caffeic acids were reported. This review further reports the presence of glycosides of quercetin, catechin and vanillic acid (Nigam et al., 2019) and it seems that a variety of dicaffeoylquinic acids are highly prevalent in *Artemisia* species. Assessment of phytoconstituents from *A. digitata* fruit pulp by LC-MS/QTOF led to the annotation of 46 compounds including protocatechuic acid, chlorogenic acid, caffeic acid, p-hydroxy-cinnamic acid, and p-hydroxybenzoic acid (Ismail et al., 2020).

Elemental composition of a carboxylated cyclohexanepolyol was shown by the presence of product ion at m/z 191.05 depicted as quinic acid. Quinic, chlorogenic and caffeic acids exhibit HIV integrase and HIV replication inhibitory effects (Choi et al., 2009). Quinic acid derivatives 3,4-di-O-caffeoylelquinic acid (3,4-diCQA) and 3,5-di-O-caffeoylelquinic acid (3,5-diCQA) inhibited the respiratory syncytial virus (RSV) with IC₅₀ values of 2.33 μM and 1.16, respectively (Li et al., 2005). Furthermore, a study on the anti-hepatitis-B virus activity of chlorogenic acid, quinic acid and caffeic acid from crude coffee extracts revealed inhibitory potency both intracellular and extracellular. In intercellular experiments, chlorogenic acid, quinic acid and caffeic acid had IC₅₀ values of 1.3, 1.6

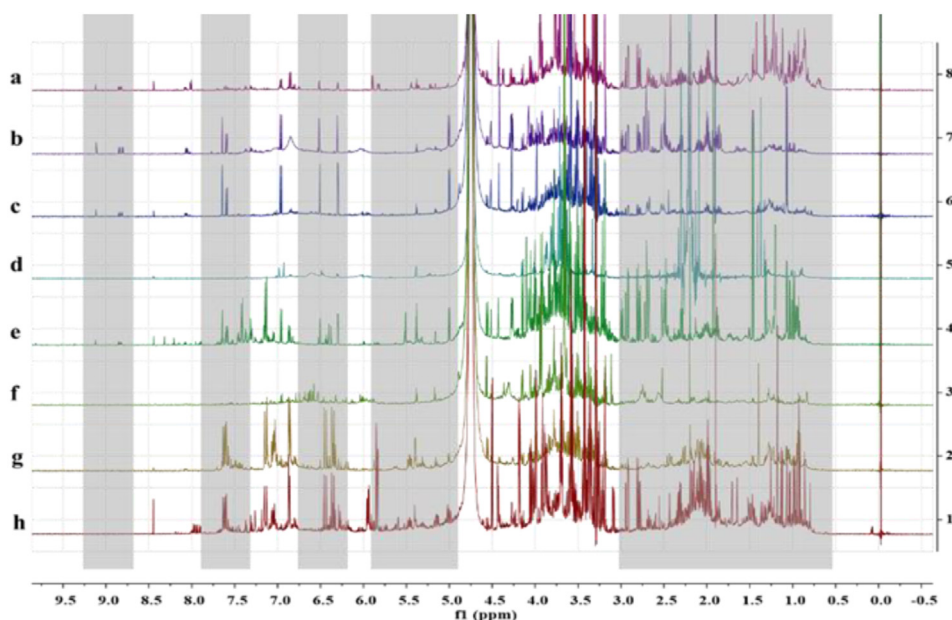


Figure 5. Stacked ¹H-NMR spectra of eight plant extracts exhibiting anti-RVFV activity. Shaded areas showing similar occurrences of metabolites. *Sutherlandia frutescens* (a), *Adansonia digitata* (b), *Elephantorrhiza elephantina* (c), *Euclea natalensis* (d), *Elaeodendron transvaalensis* (e), *Elaeodendron croceum* (f), *Helichrysum auronitens* (g) and *Artemisia afra* (h).

and 0.7 μ M, respectively. On the other hand, chlorogenic acid, quinic acid and caffeoic acid possessed IC₅₀ values of 1.2, 10.1 and 3.9 μ M when tested extracellular (Wang et al., 2009). Quinic acid was also identified in various *Helichrysum* species with anti-HIV reverse transcriptase (RT) activity, with molecular docking analysis confirming the strong binding capacity of quinic acid to the RT enzyme (Yazdi et al., 2019).

Caffeoyl types of compounds are well renowned for their antiviral activity. A study by Urushisaki et al. (2011) found that caffeoylquinic acids such as chlorogenic acid, 3,4-di-O-caffeoylelquinic acid (3,4-diCQA) and 3,5-di-O-caffeoylelquinic acid (3,5-diCQA), 4,5-di-O-caffeoylelquinic acid (4,5-diCQA), and 3,4,5-Tricaffeoylquinic acid (3,4,5-triCQA) are prominent in green propolis plants from Brazil and are potent influenza virus [(A/WSN/33 (H1N1)] inhibitors. Another study reported the presence of dicaffeoylquinic and tricaffeoylquinic acids and these compounds were prominent in the anti-HIV potent sample of *Helichrysum populifolium* (Heyman et al., 2015).

Vanillic acid was reported to be the most prominent compound in the root extract of *Rubia cordifolia* which played a significant role in the activity against rotavirus by reducing the cytopathic effect (CPE) of the virus on MA-104 cells (Sun et al., 2016). Trigonelline and ferulic acid have been reported to exhibit hypoglycaemic, hypolipidemic, neuroprotective, antimigraine, sedative, antibacterial, antiviral, and anti-tumour properties (Song et al., 2016; Mohamadi et al., 2018). Cui et al. (2013) investigated the antiviral activity of hydrogenated ferulic acid derivatives against the tobacco mosaic virus (TMV). Seven derivatives of ferulic acid showed 10.4–22.8% inhibitory percentage range which was moderate compared to positive control ribavirin with an inhibitory percentage of 32.6%. Ferulic acid does not only possess antimicrobial potency but it has shown cytoprotective activity against high glucose-induced oxidative stress in cardiomyocytes and hepatocytes. It was observed that ferulic acid at 1.5 and 10 mg/mL treatment significantly increased cell viability of hepatocytes and cardiomyocytes, and significantly decreased cell apoptosis compared with the high-glucose-treated group (Song et al., 2016).

Trigonelline is a polar hydrophilic alkaloid that has several biological activities including, hypoglycaemic, hypolipidemic, neuroprotective, antimigraine, sedative, memory-improving, antibacterial, antiviral, and antitumor activities. Furthermore, it has been implicated for being responsible for inhibiting the proliferation of viruses including herpes

simplex (type 1) virus (Özçelik et al., 2011). Li et al. (2019) evaluated the inhibitory effects of trigonelline in diabetes in rats. This study showed that trigonelline increased the body weight, inhibited the kidney weight/body ratio and reduced the blood glucose levels. Additionally, trigonelline reduced the levels of blood urea nitrogen, creatinine and albumin in type 2 diabetic rats.

The flavonoids rutin, kaempferol and a flavonol glycoside, kaempferol 3-O-rutinoside were also detected by the UPLC-qTOF-MS analysis. A review reported flavonoids as Enterovirus A71 (EV-A71) inhibitors. This review showed that kaempferol inhibits the EV-A71 sub-genotype C4 strain with an IC₅₀ value of 52.75 μ M and decreased the viral RNA copies and protein synthesis (Lalani and Poh 2020). Bioflavonoid rutin, also known as quercetin-3-rutinoside was shown by the presence of a peak at m/z 610.15. According to our analysis, rutin was found in most tested samples, except for *E. natalensis* and *E. croceum* extracts. Ganeshpurkar and Saluja (2017) documented a review on the pharmacological potential of rutin and they showed that rutin exhibits a range of biological activities including anticancer, analgesic, antiarthritic and antiviral properties. Rutin was able to inhibit the replication stage of infection with an IC₅₀ value of 110 μ M (Lalani and Poh 2020), however, it could not inhibit the viral replication of Dengue virus type-2 (DENV-2) (Keivan et al., 2014).

Other compounds that were detected include sutherlandioside A-D, and sutherlandin A-D present in *S. frutescens* which are documented for their health benefiting effects exhibiting a diverse range of biological activities such as antioxidant, anti-inflammatory, antimicrobial, anti-tumoral, anti-thrombogenic, anti-therosclerotic, anti-viral, and anti-allergic properties (Umesh and Jamsheer 2018). Quercetin-3-O-robinobioside (Q3R), kaempferol 3-O-rutinoside and rutin were detected in *A. digitata*. These three compounds have previously been reported to exhibit a range of biological activities including antiviral potency. Quercetin-3-O-robinobioside isolated from the aerial parts of *Houttuynia cordata* was evaluated using a cytopathic effect (CPE) reduction method against influenza A/WS/33 virus. From this study, Q3R showed 86 % and 66% reduction against influenza A/WS/33 virus at concentrations of 100 and 10 μ g/ml respectively (Choi et al., 2009). Quercetin 3-O-rutinoside, kaempferol 3-O-rutinoside and kaempferol, potent antiviral flavone glycosides from the leaves of *Ficus benjamina*, were reported to have strong inhibitory activity against HSV-1. These compounds

Table 3. List of compounds annotated from eight antiviral leaf extracts analysed by UHPLC-qTOF-MS showing retention times (Rt), mass-to-charge ratio (*m/z*), molecular formula, proposed metabolite and mode of detection. The table also shows in which plants were annotated metabolites present: *Artemisia afra* (Aa), *Adansonia digitata* (Ad) *Euclea natalensis* (En), *Elaeodendron croceum* (Ec), *Elaeodendron transvaalensis* (Et), *Elephantorrhiza elephantina* (Ee), *Helichrysum aureonitens* (Ha), *Sutherlandia frutescens* (Sf).

Rt (min)	Observed mass (<i>m/z</i>)	Calculated mass (<i>m/z</i>)	Fragment Ions	DBE count	Molecular Formula	Annotated Metabolites	Comments	Mode of detection	Plant species
0.93	138.0555	137.0477	110.06; 94.06	5	C ₇ H ₇ NO ₂	Trigonelline	MassBank (USA)	Positive mode	Ad, Ee, Sf
1.14	193.0488	354.0951	-	8	C ₁₆ H ₁₈ O ₉	Chlorogenic acid	Product ion; trace level	Negative mode. Ferulic fragment product (of chlorogenic acid)	Ad
2.98	353.0872	354.09508	191.1; 179.0	8	C ₁₆ H ₁₈ O ₉	3-Caffeoylquinic acid	(Clifford et al., 2008)	Negative mode	Aa, Ha
4.53	353.0872	354.09508	191.1; 179.1 (low intensity)	8	C ₁₆ H ₁₈ O ₉	5-Caffeoylquinic acid	(Clifford et al., 2008)	Negative mode	Aa, Et, Ha
4.69	353.0842	354.09508	173.0; 179.0; 191.1	8	C ₁₆ H ₁₈ O ₉	4-Caffeoylquinic acid	(Clifford et al., 2008)	Negative mode	Aa, Ha
6.03	515.1157	516.12678	353.1; 191.1; 335.1	14	C ₂₅ H ₂₄ O ₁₂	4,5-Dicaffeoylquinic acid	(Clifford et al., 2008)	Negative mode	Aa, Ha
8.87	515.1195	516.12678	173.0; 335.1	14	C ₂₅ H ₂₄ O ₁₂	3,4-Dicaffeoylquinic acid	(Clifford et al., 2008)	Negative mode	Aa, Ha
9.19	515.1196	516.12678	353.1; 191.1	14	C ₂₅ H ₂₄ O ₁₂	3,5-Dicaffeoylquinic acid	(Clifford et al., 2008)	Negative mode	Aa, Ha
10.14	193.0488	194.0579	-	6	C ₁₀ H ₁₀ O ₄	Ferulic acid	NIST 2014; product ion	Negative mode. Ferulic fragment product (of chlorogenic acid)	Aa, Ha
1.14	167.0325	168.0423	-	5	C ₈ H ₈ O ₄	Vanillic acid	Product ion	Negative mode	Et
2.50	315.1063	316.1158	153.05	5	C ₁₄ H ₂₀ O ₈	Hydroxytyrosol glucoside/^ vanilloidoside	Mass Fragment	Negative mode	Et
2.60	153.0546	152.0473	-	5	C ₈ H ₈ O ₃	4-Hydroxyphenylacetate/vanillin	Product ion	positive mode	Et
1.34	191.0546	192.0634	173.0; 128.0; 111.0	2	C ₇ H ₁₂ O ₆	Quinic acid	MAGMa, KEGG/HMDB/PubChem	Negative mode	Aa, Ad, Et, Ha
23.74	293.2116	294.2195	-	4	C ₁₈ H ₃₀ O ₃	13S-Hydroxy-9Z,11E,15Z-octadecatrienoic acid	MAGMa, KEGG/HMDB/PubChem	Negative mode	Aa, Ad, En, Ec, Et, Ee, Ha, Sf
24.76	295.2274	296.23514	-	3	C ₁₈ H ₃₂ O ₃	13-Hydroxy-9Z,11E-octadecadienoic acid	MAGMa, KEGG/HMDB/PubChem	Negative mode	Aa, Ad, En, Ec, Et, Ee, Ha, Sf
2.12	166.0833	165.0790	120.1	5	C ₉ H ₁₁ NO ₂	Phenylalanine	NIST 2014	Positive mode	Aa, Ad, Ee, Ha, Sf
3.27	205.0968	204.0899	188.1; 159.1; 146.1	7	C ₁₁ H ₁₂ N ₂ O ₂	L-Tryptophan	NIST 2014	Positive mode	Aa, Ad, Ee, Ha, Sf
12.23	301.0305	302.0427	273.04; 178.99; 151.00	11	C ₁₅ H ₁₀ O ₇	Quercetin	NIST 2014 & User Library	Negative mode	Ee
5.12	771.1982	772.2062	609.1; 462.1; 301.0	14	C ₃₃ H ₄₀ O ₂₁	Quercetin 3-rutinoside-7-glucoside	MAGMa, KEGG/HMDB/PubChem	Negative mode	Ad
8.24	609.1454	610.1534	300.02	13	C ₂₇ H ₃₀ O ₁₆	Rutin	NIST 2014	Negative mode	Aa, Ad, Ec, Et, Ee, Ha, Sf
8.24	609.1438	610.1534	300.02	13	C ₂₇ H ₃₀ O ₁₆	Rutin hydrate	Reference standard; NIST 2014	Negative mode	Aa, Et, Ha
9.33	593.1509	594.1585	285.0	13	C ₂₇ H ₃₀ O ₁₅	Kaempferol 3-O-rutinoside	MAGMa, KEGG/HMDB/PubChem	Negative mode	Aa, Ad, Et
14.18	285.0374	286.0477	-	11	C ₁₅ H ₁₀ O ₆	Kaempferol	NIST 2014	Negative mode	Aa, Ad, En, Et, Ee
3.76	307.0763	306.0740	289.07; 181.05; 139.04	8	C ₁₅ H ₁₄ O ₇	Epigallocatechin	NIST 2014; MassFragment	Positive mode	Ec
4.15	289.0716	290.0790	245.08; 205.05; 179.03	9	C ₁₅ H ₁₄ O ₆	Catechin	NIST 2014 & mzCloud	Negative mode	En, Ee
4.23	289.0692	290.0790	245.08; 205.05; 179.03	9	C ₁₅ H ₁₄ O ₆	Epi-catechin	NIST 2014 & mzCloud	Negative mode	En, Ee
4.31	319.0769	320.0896	289.07	9	C ₁₆ H ₁₆ O ₇	4'-O-Methyl-(-)epigallocatechin	Yelani et al., 2010; Yelani and Meyer 2009	Negative mode	En

(continued on next page)

Table 3 (continued)

Rt (min)	Observed mass (<i>m/z</i>)	Calculated mass (<i>m/z</i>)	Fragment Ions	DBE count	Molecular Formula	Annotated Metabolites	Comments	Mode of detection	Plant species
8.24	463.0845	464.0955	316.02	12	C ₂₁ H ₂₀ O ₁₂	Myricitrin	NIST 2014	Negative mode	En
6.06	591.1492	592.1581	-	18	C ₃₁ H ₂₈ O ₁₂	Proanthocyanidin A	DNP & KnapSack	Negative mode	Ec
10.37	435.1311	436.1370	273.08; 167.03; 125.04	10	C ₂₁ H ₂₄ O ₁₀	Phlorizin	NIST 2014	Negative mode	Ec
11.20	317.0673	316.0583	302.04; 285.04; 153.02	11	C ₁₆ H ₁₂ O ₇	Isorhamnetin	NIST 2014	Positive mode	En
13.52	271.0608	272.0685	151.00	10	C ₁₅ H ₁₂ O ₅	Naringenin	Yelani et al., 2010; Yelani and Meyer 2009 NIST 2014 User Lib	Negative mode	En, Ec
6.04	319.0833	320.0896	-	9	C ₁₆ H ₁₆ O ₇	Ourateacatechin/4-methyl-epigallocatechin	KnapSack	Negative mode	Ec
14.11	285.0400	286.0477	-	11	C ₁₅ H ₁₀ O ₆	Luteolin	MAGMa, KEGG/ HMDB/PubChem	Negative mode	Et
7.61	609.1436	610.1534	447.09; 285.04	13	C ₂₇ H ₃₀ O ₁₆	Luteolin diglycoside	MAGMa, KEGG/ HMDB/PubChem	Negative mode	Et
10.40	447.0905	448.1006	285.04	12	C ₂₁ H ₂₀ O ₁₁	Luteolin glycoside	NIST 2014;	Negative mode	Et
3.43	577.1331	578.1424	451.10; 425.08; 407.07; 289.07	18	C ₃₀ H ₂₆ O ₁₂	Procyanidin B2/B5	NIST 2014 & MassBank (USA)	Negative mode	Ee
9.31	593.1516	594.1585	285.04	13	C ₂₇ H ₃₀ O ₁₅	Nicotiflorin/kaempferol-glucoside-rhamnoside	NIST 2014 & User Library	Negative mode	Aa, Ee, Ec
24.90	429.3640	428.3654	-	5	C ₂₉ H ₄₈ O ₂	Elaeodendrol	Product ion	Positive mode	Et
16.27	651.4096	652.41865	-	7	C ₃₆ H ₆₀ O ₁₀	Sutherlandioside A	Avula et al., 2010; DNP	Negative mode	Sf
15.35	651.4105	652.41865	-	7	C ₃₆ H ₆₀ O ₁₀	Sutherlandioside B	Avula et al., 2010; DNP	Negative mode	Sf
16.39	649.3954	650.40300	-	8	C ₃₆ H ₅₈ O ₁₀	Sutherlandioside C	Avula et al., 2010; DNP	Negative mode	Sf
16.42	633.4003	634.40808	-	8	C ₃₆ H ₅₈ O ₉	Sutherlandioside D	Avula et al., 2010); DNP	Negative mode	Sf
10.78	539.1742	540.1843	377.12; 345.09; 307.08; 275.09	10	C ₂₅ H ₃₂ O ₁₃	Oleuropein/oleurosides	NIST 2014; MassFragment	Negative mode	Et
9.43	701.2298	702.2371	539.19; 377.12; 307.08; 275.08	11	C ₃₁ H ₄₂ O ₁₈	Oleuropeinyl monoglucoside	MAGMa, KEGG/ HMDB/PubChem	Negative mode	Et
11.51	539.1710	540.1843	377.12; 345.09; 307.08; 275.09	10	C ₂₅ H ₃₂ O ₁₃	Oleuropein/oleurosides	NIST 2014; MassFragment	Negative mode	Et
4.37	603.2842	602.2727	471.24; 441.23; 309.18	12	C ₃₂ H ₄₂ O ₁₁	Plantagiolide	DNP	positive mode	Ec
12.42	535.2904	536.2985	373.24; 161.04	8	C ₂₉ H ₄₄ O ₉	Digitoxigenin glucoside	Prinsloo and Meyer (2007)	Negative mode	Ec
12.16	533.2751	532.2672	515.26; 387.321; 369.20; 351.19	10	C ₂₉ H ₄₀ O ₉	corotoxigenin-rhamnopyroside	DNP & KnapSack	Positive mode	Ec
16.10	377.0972	376.0947	359.09; 345.11	15	C ₂₂ H ₁₆ O ₆	Natalenone/naphthoherinarin	DNP	Positive mode	En
8.27	739.1750	740.17999	637.15; 595.13; 300.03	15	C ₃₂ H ₃₆ O ₂₀	Sutherlandin A	Avula et al. (2010); DNP	Negative mode	Sf
8.60	739.1724	740.17999	637.15; 595.13; 300.03	15	C ₃₂ H ₃₆ O ₂₀	Sutherlandin B	Avula et al. (2010); DNP	Negative mode	Sf
9.23	723.1805	724.18508	621.15; 579.13; 284.03	15	C ₃₂ H ₃₆ O ₁₉	Sutherlandin C	Avula et al. (2010); DNP	Negative mode	Sf
9.46	723.1805	724.18508	621.15; 579.13; 284.03	15	C ₃₂ H ₃₆ O ₁₉	Sutherlandin D	Avula et al. (2010); DNP	Negative mode	Sf

(continued on next page)

Table 3 (continued)

Rt (min)	Observed mass (m/z)	Calculated mass (m/z)	Fragment Ions	DBE count	Molecular Formula	Annotated Metabolites	Comments	Mode of detection	Plant species
8.27	739.1750	740.17999	637.15; 595.13; 300.03	15	C ₃₂ H ₃₆ O ₂₀	Sutherlandin A	Avula et al. (2010); DNP	Negative mode	Sf
6.27	431.1926	432.1941	-	5	C ₁₉ H ₃₀ O ₈	Roseoside	FA adduct	Negative mode	En
7.34	625.1299	626.1483	479.08; 463.08; 316.02	13	C ₂₇ H ₃₀ O ₁₇	Myricetin-3-neohesperidoside	MAGMa, KEGG/HMDB/PubChem	Negative mode	En
9.63	477.0996	478.1111	447.09; 331.05; 316.02	21	C ₂₂ H ₂₂ O ₁₂	Estragonoside	MAGMa, KEGG/HMDB/PubChem	Negative mode	En
9.69	447.0910	448.1006	301.04	12	C ₂₁ H ₂₀ O ₁₁	Quercitrin	MAGMa, KEGG/HMDB/PubChem	Negative mode	En
10.16	965.2995	966.3064	671.20	9	C ₃₇ H ₅₈ O ₂₉	Lipid	MAGMa, KEGG/HMDB/PubChem	Negative mode	En
11.12	677.4996	678.5071	461.11	6	C ₄₀ H ₇₀ O ₈	Lipid	MAGMa, KEGG/HMDB/PubChem	Negative mode	En

exhibited EC₅₀ values of 1.5, 3.0, 0.9 and 25.0 μM, respectively, with the positive control acyclovir having an EC₅₀ value of 0.1 μg/mL (Yarmolinsky et al., 2012).

As all the selected plants have previously reported anti-viral activity, the multitude of compounds with known anti-viral activity could be expected. However, in this study, the presence of two hydroxylated fatty acids were annotated for the first time in all the anti-viral active samples and are reported as 13S-Hydroxy-9Z,11E,15Z-octadecatrienoic acid and 13-Hydroxy-9Z,11E-octadecadienoic acid with UPLC-qTOF-MS analysis. Additionally, the NMR peak regions of this compound at 1.3, 2.0, 2.2 and 2.3 ppm in the aliphatic region, 3.9, 5.5, 5.6 and 5.8 ppm in the sugar region and 6.0 and 6.2 ppm in the aromatic region matched very well to the positively associated NMR regions in the contribution plot (Figure 4), supporting the presence of these compounds in the active anti-RVFV samples. Kaigongi et al. (2020) reported for the first time the presence of the unsaturated fatty acid, 17-hydroxylinolenic acid from a multi-purpose medicinal plant *Dodonaea viscosa* Jacq (Sapindaceae) and has significant pharmacological activities ranging from antimicrobial, anti-inflammatory, anti-allergic and anticancer activities (Mundt et al., 2003; Korinek et al., 2017). The antiviral activity of various naturally occurring fatty acids has been demonstrated. Fatty acids, particularly the medium chain saturated fatty acids and long chain unsaturated fatty acids were reported to be able to reduce viral concentrations of vesiculovirus (VSV) and herpes simplex virus (HSV) in cell cultures by 10,000 fold (Aldridge, 2020). Another oxygenated fatty acid, 10S, 17S-dihydroxydocosahexaenoic acid, also known as protectin-D1 (PD1) has been shown to inhibit the H5N1 influenza virus replication by interfering with the virus RNA nuclear export. Protectin-D1 (PD1) exhibited a 30 % reduction of the viral load with a TCID₅₀ = 1 × 10⁵ (Morita et al., 2013). Hydroxy polyunsaturated fatty acids have been shown to possess anti-viral activity (Riccio et al., 2020) and a particular mechanism of action includes the interference with the binding ability of the virus to host cell receptors thereby decreasing the viral load (Rita et al., 2018). Furthermore, a fatty acid methyl ester [(9Z, 11E)-13hydroxy-9,11-octadecadienoic acid and (9Z,11E)13-oxo-9,11-octadecadienoic acid] isolated from leaves and twigs of *Ehretia dicksonii* possessed anti-inflammatory activity on mouse ears and lipoxygenase inhibitory activities of 63% and 79% were observed, respectively (Dong et al., 2000). The antiviral assessment of *Phyllocaulis boraceiensis* mucus and its fractions against influenza A strain using Madin–Darby canine kidney (MDCK) cells revealed that the mucus and fractions reduced the viral-induced cytopathic effects and viral replication by more than 80%. HPLC-DAD-ESI-MS/MS analysis of *P. boraceiensis* mucus and its fractions showed the presence of hydroxy polyunsaturated fatty acids related to the 17-hydroxylinolenic acid as major antiviral constituents. This deduces that the hydroxy polyunsaturated fatty acids obtained interfere with the binding ability of the

virus to host cell receptors thereby decreasing the viral load (Rita et al., 2018). The presence of the two hydroxylated fatty acids in all the samples, showing anti-RVFV activity, is therefore very likely to be major contributors to the activity.

5. Conclusion

NMR-based metabolomics coupled with multivariate statistical analysis and UHPLC-TOF/MS was used to profile metabolites from the anti-RVFV medicinal plants. The PCA and HCA were used to show an overview of groupings, outliers and clustering trends, while the OPLS-DA discriminated the active and less-active samples. A number of compounds identified in the samples with anti-RVFV activity have been proven to be potent anti-viral compounds in various studies. This is also supported by the subsequent molecular docking reports and mechanism of action, proving the potential of these compounds to affect viral infection. This study is also the first reporting two hydroxylated fatty acids common in the all the active samples, namely, 13-Hydroxy-9Z,11E-octadecadienoic acid and 13S-Hydroxy-9Z,11E,15Z-octadecatrienoic acid. These two compounds, for the first time reported in the plants with anti-RVFV activity, were shown by the peaks at *m/z* 295.2274 and *m/z* 293.2116, respectively. The application of metabolomics has therefore shown its ability to rapidly identify significant metabolites in a mixture within a plant sample and among eight antiviral plants. Isolation of the active components highlighted in this study should be further investigated for their anti-RVFV potential as individual compounds, but also the possible synergistic effects with additional anti-viral compounds present in the active plants, which might provide insight into their contributing role in anti-RVFV activity.

Declarations

Author contribution statement

Jacques Vervoort and Gerhard Prinsloo: Conceived and designed the experiments; Analyzed and interpreted the data.

Garland K. More: Conceived and designed the experiments; Performed the experiments; Analyzed and interpreted the data; Wrote the paper.

Paul Steenkamp: Analyzed and interpreted the data; Contributed reagents, materials, analysis tools or data.

Funding statement

This work was supported by the College of Agriculture and Environmental Science and University of South Africa Institutional Masters & Doctoral funding.

Data availability statement

Data included in article/supplementary material/referenced in article.

Declaration of interests statement

The authors declare no conflict of interest.

Additional information

Supplementary content related to this article has been published online at <https://doi.org/10.1016/j.heliyon.2022.e08936>.

Acknowledgements

Dr Olusola Bodede (Post-doctoral fellow, UNISA), and Dr Fidele Tugizimana (University of Johannesburg) for their support.

References

- Al-youssef, H.M., Hassan, W.H.B., 2014. Phytochemical and pharmacological aspects of *Carissa edulis* Vahl: a review. *Arab. J. Chem.* 10 (1), 109–113.
- Asres, K., Bucar, F., Kartnig, T., Witvrouw, M., Pannecouque, C., De Clercq, E., 2001. Antiviral activity against human immunodeficiency virus type 1 (HIV-1) and type 2 (HIV-2) of ethnobotanically selected Ethiopian medicinal plants. *Phytother Res.* 15 (1), 62–69.
- Avula, B., Wang, Y.H., Smillie, T.J., Fu, X., Li, X.C., Mabusela, W., Syce, J., Johnson, Q., Folk, W., Khan, I.A., 2010. Quantitative determination of flavonoids and cycloartanol glycosides from aerial parts of *Sutherlandia frutescens* (L.) R. BR. by using LC-UV/ELSD methods and confirmation by using LC-MS method. *J. Pharmaceut. Biomed. Anal.* 52 (2), 173–180.
- Bagley, M.A., 2018. Toward an Effective Indigenous Knowledge protection Regime Case Study of South Africa. CIGI Papers No. 207. <https://www.cigionline.org/publications/toward-effective-indigenous-knowledge-protection-regime-case-study-South-Africa>.
- Bessong, P.O., Obi, C.L., Andréola, M.L., Rojas, L.B., Pouységuy, L., Igumbor, E., Meyer, J.J.M., Quideau, S., et al., 2005. Evaluation of selected South African medicinal plants for inhibitory properties against human immunodeficiency virus type 1 reverse transcriptase and integrase. *J. Ethnopharmacol.* 99 (1), 83–91.
- Bessong, P.O., Rojas, L.B., Obi, L.C., Tshisikawe, P.M., Igumbor, E.O., 2006. Further screening of Venda medicinal plants for activity against HIV type 1 reverse transcriptase and integrase. *Afr. J. Biotechnol.* 5 (6), 526–528.
- Chen, W., Van Wyk, B.E., Vermaak, I., Viljoen, A.M., 2012. Cape aloes - a review of the phytochemistry, pharmacology and commercialisation of *Aloe ferox*. *Phytochem. Lett.* 5 (1), 1–12.
- Chen, J., Liu, Z., Fan, S., Yang, D., Zheng, P., Shao, W., Qi, Z., Xu, X., et al., 2014. Combined application of NMR- and GC-MS-Based metabolomics yields a superior urinary biomarker panel for bipolar disorder. *Sci. Rep.* 4, 1–6.
- Choi, Y.H., Verpoorte, R., 2014. Metabolomics: what you see is what you extract. *Phytochem. Anal.* 25 (4), 289–290.
- Choi, H.J., Song, J.H., Park, K.S., Kwon, D.H., 2009. Inhibitory effects of quercetin 3-rhamnoside on influenza A virus replication. *Eur. J. Pharmaceut. Sci.* 37 (3–4), 329–333.
- Clifford, M.N., Kirkpatrick, J.O., Kuhnert, N., Rozendaal, H., Salgado, P.R., 2008. LC-MSn analysis of the cis isomers of chlorogenic acids. *Food Chem.* 106 (1), 379–385.
- Cui, C., Wang, Z.P., Du, X.J., Wang, L.Z., Yu, S.J., Liu, X.H., Li, Z.M., Zhao, W.G., 2013. Synthesis and antiviral activity of hydrogenated ferulic acid derivatives. *J. Chem.* 2013, 1–5.
- Dhanani, T., Singh, R., Kumar, S., 2016. Extraction optimization of gallic acid, (+)-catechin, procyanidin-B2, (-)-epicatechin, (-)-epigallocatechin gallate, and (-)-epicatechin gallate: their simultaneous identification and quantification in *Saraca asoca*. *J. Food Drug Anal.* 25 (3), 691–698.
- Ding, Y., Cao, Z., Cao, L., Ding, G., Wang, Z., Xiao, W., 2017. Antiviral activity of chlorogenic acid against influenza A (H1N1/H3N2) virus and its inhibition of neuraminidase. *Sci. Rep.* 7, 1–11.
- Dong, M., Oda, Y., Hirota, M., 2000. (10E,12Z,15Z)-9-hydroxy-10,12,15-octadecatrienoic acid methyl ester as an anti-inflammatory compound from *Ehretia dicksonii*. *Biosci. Biotechnol. Biochem.* 64 (4), 882–886.
- El-Toumy, S.A., Salib, J.Y., El-Kashash, W.A., Marty, C., Bedoux, G., Bourgougoun, N., 2018. Antiviral effect of polyphenol rich plant extracts on herpes simplex virus type 1. *Food Sci. Human Wellness* 7 (1), 91–101.
- Emwas, A.H., Roy, R., McKay, R.T., Tenori, L., Saccenti, E., Nagana Gowda, G.A., Raftery, D., Alahmari, F., et al., 2019. NMR spectroscopy for metabolomics research. *Metabolites* 9 (7).
- Feustel, S., Ayón-Pérez, F., Sandoval-Rodríguez, A., Rodríguez-Echevarría, R., Contreras-Salinas, H., Armendáriz-Borunda, J., Sánchez-Orozco, L.V., 2017. Protective effects of *Moringa oleifera* on HBV genotypes C and H transiently transfected Huh7 Cells. *J. Immunol. Res.* 2017, 1–9.
- Ganeshpurkar, A., Saluja, A.K., 2017. The pharmacological potential of rutin. *Saudi Pharmaceut. J.* 25 (2), 149–164.
- Hafidh, R.R., Abdulamir, A.S., Jahanshiri, F., Abas, F., Abu-Bakar, F., Sekawi, Z., 2009. Asia is the mine of natural antiviral products for public health. *Open Compl. Med. J.* 1, 58–68.
- Harnett, S.M., Oosthuizen, V., Van De Venter, M., 2005. Anti-HIV activities of organic and aqueous extracts of *Sutherlandia frutescens* and *Lobostemon trigonus*. *J. Ethnopharmacol.* 96 (1–2), 113–119.
- Heyman, M., Senejoux, F., Seibert, I., Klimkait, T., Jaichand, V., Meyer, M., 2015. Identification of anti-HIV active dicaffeoylquinic- and tricaffeoylquinic acids in *Helichrysum populifolium* by NMR-based metabolomic guided fractionation. *Fitoterapia* 103, 155–164.
- Hurinanthan, V., 2013. Anti-HIV Activity of Selected South African Medicinal Plants. PhD Thesis. Department of Biotechnology and Food Technology, Durban University of Technology, Durban, South Africa. https://openscholar.dut.ac.za/bitstream/10321/916/1/Hurinanthan_2013.pdf.
- Ismail, B.B., Pu, Y., Guo, M., Ma, X., Liu, D., 2020. LC-MS/QTOF identification of phytochemicals and the effects of solvents on phenolic constituents and antioxidant activity of baobab (*Adansonia digitata*) fruit pulp LC-MS/QTOF identification of phytochemicals and the effects of solvents on phenol. *Food Chem.* 277, 279–288.
- Karimi, A., Majlesi, M., Rafieian-kopaei, M., 2015. Herbal versus synthetic drugs; beliefs and facts. *J. Nephropharmacol.* 4 (1), 27–30.
- Keivan, Z., Boon-Teong, T., Sing-Sin, S., Pooi-Fong, W., Mohd, R.M., Sazaly, A., 2014. In vitro antiviral activity of fisetin, rutin and naringenin against dengue virus type-2. *J. Med. Plants Res.* 8 (6), 307–312.
- Klos, M., van de Venter, M., Milne, P.J., Traore, H.N., Meyer, D., Oosthuizen, V., 2009. In vitro anti-HIV activity of five selected South African medicinal plant extracts. *J. Ethnopharmacol.* 124 (2), 182–188.
- Korinek, M., Tsai, Y., El-shazly, M., Lai, K., Chen, B., 2017. Anti-allergic Hydroxy fatty acids from *Typhonium blumei* explored through ChemGPS-NP. *Front. Pharmacol.* 8 (356), 1–7.
- Lalani, S., Poh, C.L., 2020. Flavonoids as antiviral agents for enterovirus A71 (EV-A71). *Viruses* 12 (2), 1–32.
- Lall, N., Kishore, N., Bodiba, D., More, G., Tshikalange, E., Kikuchi, H., Oshima, Y., 2017. Alkaloids from aerial parts of *Annona senegalensis* against *Streptococcus mutans*. *Nat. Prod. Res.* 31 (16), 1944–1947.
- Lawal, U., Maulidiani, M., Shaari, K., Ismail, I.S., Khatib, A., Abas, F., 2017. Aspects of plant biology discrimination of *Ipomoea aquatica* cultivars and bioactivity correlations using NMR-based metabolomics approach. *Plant Biosyst. Int. J. Deal. Aspect. Plant Biol.* 151 (5), 1–11.
- Li, Y., But, P.P.H., Ooi, V.E.C., 2005. Antiviral activity and mode of action of caffeoquinic acids from *Schefflera heptaphylla* (L.) Frodin. *Antivir. Res.* 68 (1), 1–9.
- Li, Y., Li, Q., Wang, C., Lou, Z., Li, Q., 2019. Trigonelline reduced diabetic nephropathy and insulin resistance in type-2 diabetic rats through peroxisome proliferator-activated receptor- γ . *Exp. Ther. Med.* 18 (2), 1331–1337.
- Lipipun, V., Kurokawa, M., Suttisri, R., Taweechotipat, P., Pramyothin, P., Hattori, M., Shiraki, K., 2003. Efficacy of Thai medicinal plant extracts against herpes simplex virus type 1 infection in vitro and in vivo. *Antivir. Res.* 60 (3), 175–180.
- Liu, N.Q., Van der Kooy, F., Verpoorte, R., 2009. *Artemisia afra*: a potential flagship for African medicinal plants? *South Afr. J. Bot.* 75 (2), 185–195.
- Lunat, I., 2011. Traditional, Complementary and Alternative Medicine Use in HIV-positive Patients Magister of Pharmaciae. Thesis. Nelson Mandela Metropolitan University (NMMU), Port Elizabeth, Eastern Cape, South Africa.
- Meyer, J.J.M., Afolayan, A.J., Taylor, M.B., Erasmus, D., 1997. Antiviral activity of galangin isolated from the aerial parts of *Helichrysum aureonitens*. *J. Ethnopharmacol.* 56 (2), 165–169.
- Mohamadi, N., Sharififar, F., Pournamdar, M., Ansari, M., 2018. A Review on biosynthesis, analytical techniques, and pharmacological activities of trigonelline as a plant alkaloid. *J. Diet. Suppl.* 15 (2), 207–222.
- Mohana, C.N., Yashavantha Rao, H.C., Rakshit, D., Mithun, P.R., Nuthan, B.R., Satish, S., 2018. Omics based approach for biodiscovery of microbial natural products in antibiotic resistance era. *J. Genetic Eng. Biotechnol.* 16 (1), 1–8.
- More, G.K., Makola, R.T., Prinsloo, G., 2021. In vitro evaluation of anti-Rift Valley Fever Virus, antioxidant and anti-inflammatory activity of South African medicinal plant extracts. *Viruses* 13 (221), 1–18.
- Morita, M., Kuba, K., Ichikawa, A., Nakayama, M., Katahira, J., Iwamoto, R., 2013. The lipid mediator protectin D1 inhibits influenza virus replication and improves severe influenza. *Cell* 153 (1), 112–125.
- Mukhtar, M., Arshad, M., Ahmad, M., Pomerantz, R.J., Wigdahl, B., Parveen, Z., 2008. Antiviral potentials of medicinal plants. *Virus Res.* 131 (2), 111–120.
- Mundt, S., Kreitlow, S., Jansen, R., 2003. Fatty acids with antibacterial activity from the cyanobacterium *Oscillatoria redekei* HUB 051. *J. Appl. Phycol.* 15, 263–267.
- Naveed, M., Hejazi, V., Abbas, M., Kamboh, A.A., Khan, G.J., Shumzaid, M., Ahmad, F., Babazadeh, D., et al., 2018. Chlorogenic acid (CGA): a pharmacological review and call for further research. *Biomed. Pharmacother.* 97, 67–74.
- Nigam, M., Atanassova, M., Mishra, A.P., Pezzani, R., Devkota, H.P., Plygun, S., Salehi, B., 2019. Bioactive compounds and health benefits of *Artemisia* species. *Natural Product Commun.* 1–17.
- The National Institute of Standards and Technology (NIST), 2014. Standard Reference Database 69: *NIST Chemistry WebBook*. <https://webbook.nist.gov/cgi/cbook.cgi?ID=C537984&Mask=200#Refs>.
- Özçelik, B., Kartal, M., Orhan, I., 2011. Cytotoxicity, antiviral and antimicrobial activities of alkaloids, flavonoids, and phenolic acids. *Pharmaceut. Biol.* 49 (4), 396–402.
- Prinsloo, G., Meyer, J.J.M., 2007. Isolation of an Anti-HIV Compound from *Elaeodendron Croceum* (Thunb.) DC. Department of Botany, Faculty of Natural and Agricultural Sciences. University of Pretoria. Philosophiae Doctorae Thesis. <https://repository.up.ac.za/bitstream/handle/2263/25336/Complete.pdf?sequence=10>.

- Prinsloo, G., Vervoort, J., 2018. Identifying anti-HSV compounds from unrelated plants using NMR and LC-MS metabolomic analysis. *Metabolomics* 14 (10), 1–7.
- Prinsloo, G., Meyer, J.J.M., Hussein, A.A., Munoz, E., Sanchez, R., 2010. A cardiac glucoside with invitro anti-HIV activity isolated from *Elaeodendron croceum*. *Nat. Prod. Res.* 24 (18), 1743–1746.
- Quansah, E., Karikari, T.K., 2016. Phytochemistry letters potential role of metabolomics in the improvement of research on traditional African medicine. *Phytochem. Lett.* 17, 270–277.
- Rathore, B., Ali Mahdi, A., Nath Paul, B., Narayan Saxena, P., Kumar Das, S., 2007. Indian herbal medicines: possible potent therapeutic agents for rheumatoid arthritis. *J. Clin. Biochem. Nutr.* 41 (1), 12–17.
- Riccio, G., Ruocco, N., Mutalipassi, M., Costantini, M., Zupo, V., Coppola, D., de Pascale, D., Lauritano, C., 2020. Ten-year research update review: antiviral activities from marine organisms. *Biomolecules* 10 (7), 1–36.
- Rita, A., Piza, D.T., Isabel, M., Giuseppina, D.O., Ronaldo, N., Mendonça, Z., Figueiredo, C.A., 2018. Polyunsaturated fatty acids from *Phyllocaulis boraceiensis* mucus block the replication of influenza virus. *Arch. Microbiol.* 200 (6), 961–970.
- Sharma, A., Rangari, V., 2016. HIV-1 reverse transcriptase and protease assay of methanolic extracts of *Adansonia digitata* L. *Int. J. Pharm. Pharmaceut. Sci.* 8 (9), 124–127.
- Sigidi, M.T., Traoré, A.N., Boukandou, M.M., Tshisikhawe, M.P., Ntuli, S.S., Potgieter, N., 2017. Anti-HIV, pro-inflammatory and cytotoxicity properties of selected Venda plants. *Indian J. Traditio. Knowl.* 16 (4), 545–552.
- Silva, O., Barbosa, S., Diniz, A., Valdeira, M.L., Gomes, E., 1997. Plant extracts with antiviral activity against Herpes simplex virus type 1 and African swine fever virus. *Int. J. Pharmacogn.* 35, 12–16.
- Song, Y., Wen, L., Sun, J., Bai, W., Jiao, R., Hu, Y., Peng, X., He, Y., et al., 2016. Cytoprotective mechanism of ferulic acid against high glucose-induced oxidative stress in cardiomyocytes and hepatocytes. *Food Nutr. Res.* 60, 1–9.
- Sulaiman, L.K., Oladele, O.A., Shittu, I.A., Emikpe, B.O., Oladokun, A.T., Meseko, C.A., 2011. In-ovo evaluation of the antiviral activity of methanolic root-bark extract of the African Baobab (*Adansonia digitata* Lin). *Afr. J. Biotechnol.* 10 (20), 4256–4258.
- Sun, Y., Gong, X., Tan, J.Y., Kang, L., Li, D., Robinet, E., Gil, C., 2016. In Vitro Antiviral Activity of *Rubia cordifolia* Aerial Part Extract against Rotavirus Preparation of Extract, 7, pp. 1–10.
- Tabassum, N., Lee, J., Yim, S., Batkhuu, G.J., Jung, D., Williams, D.R., 2016. Isolation of 4,5-O-Dicaffeoylquinic acid as a pigmentation inhibitor Occurring in *Artemisia capillaris* Thunberg and its validation in vivo. *Evid. base Compl. Alternative Med.* 2016, 1–11.
- Terasaki, K., Murakami, S., Lokugamage, K.G., Makino, S., 2011. Mechanism of tripartite RNA genome packaging in Rift Valley fever virus. *Proc. Natl. Acad. Sci. Unit. States Am.* 108 (2), 804–809.
- Theo, A., Masebe, T., Suzuki, Y., Kikuchi, H., Wada, S., Obi, C.L., Bessong, P.O., Usuzawa, M., et al., 2009. *Peltophorum africanum*, a traditional South African medicinal plant, contains an anti-HIV-1 constituent, betulinic acid. *Tohoku J. Exp. Med.* 217 (2), 93–99.
- Tolo, F.M., Rukunga, G.M., Muli, F.W., Njagi, E.N.M., Njue, W., Kumon, K., Mungai, G.M., Muthaura, C.N., et al., 2006. Anti-viral activity of the extracts of a Kenyan medicinal plant *Carissa edulis* against herpes simplex virus. *J. Ethnopharmacol.* 104 (1–2), 92–99.
- Tolo, F., Rukunga, G., Muli, F., Ochora, J., Eizuru, Y., 2007. In vitro anti-viral activity of aqueous extracts of Kenyan *Carissa edulis*, *Prunus africana* and *Melia azedarach* against human cytomegalovirus. *Afr. J. Health Sci.* 14 (3), 143–148.
- Tshikalange, T.E., Meyer, J.J.M., Lall, N., Muñoz, E., Sancho, R., Van de Venter, M., Oosthuizen, V., 2008. In vitro anti-HIV-1 properties of ethnobotanically selected South African plants used in the treatment of sexually transmitted diseases. *J. Ethnopharmacol.* 119 (3), 478–481.
- Umesh, C.V., Jamsheer, A.M., 2018. The role of flavonoids in drug discovery - review on potential applications. *Res. J. Life Sci. Bioinform. Pharmaceut. Chem. Sci.* 4 (70), 1–8.
- Urushisaki, T., Takemura, T., Tazawa, S., Fukuoka, M., Hosokawa-muto, J., Araki, Y., Kuwata, K., 2011. Caffeoylquinic acids are major constituents with potent anti-influenza effects in Brazilian green propolis water extract. *Evid. base Compl. Alternative Med.* 2011.
- Urvinder, K.S., Oyeyemi, B.F., Shet, A., Gopalan, B.P., Himanshu, D., Bhavesh, N.S., Tandon, R., 2020. Plasma metabolomic study in perinatally HIV-infected children using 1H NMR spectroscopy reveals perturbed metabolites that sustain during therapy. *PLoS One* 15 (8), 1–17.
- Vrieling, F., Alisjahbana, B., Sahiratmadja, E., van Crevel, R., Harms, A.C., Hankemeier, T., Ottenhoff, T.H.M., Joosten, S.A., 2019. Plasma metabolomics in tuberculosis patients with and without concurrent type 2 diabetes at diagnosis and during antibiotic treatment. *Sci. Rep.* 9 (1), 1–12.
- Wang, G.F., Shi, L.P., Ren, Y.D., Liu, Q.F., Liu, H.F., Zhang, R.J., Li, Z., Zhu, F.H., et al., 2009. Anti-hepatitis B virus activity of chlorogenic acid, quinic acid and caffeic acid in vivo and in vitro. *Antivir. Res.* 83 (2), 186–190.
- Wintola, O.A., Sunmonu, T.O., Afolayan, A.J., 2010. The effect of *Aloe ferox* Mill. In the treatment of loperamide-induced constipation in Wistar rats. *BMC Gastroenterol.* 10 (95).
- Woalder, 2015. A new golden age of natural products drug discovery. *Cell* 163 (6), 1297–1300.
- Yarmolinsky, L., Huleihel, M., Zaccai, M., Ben-Shabat, S., 2012. Potent antiviral flavone glycosides from *Ficus benjamina* leaves. *Fitoterapia* 83 (2), 362–367.
- Yazdi, S.E., Prinsloo, G., Heyman, H.M., Oosthuizen, C.B., Klimkait, T., Meyer, J.J.M., 2019. Anti-HIV-1 reverse transcriptase activity of quinic acid isolated from *Helichrysum mimites* using NMR-based metabolomics and computational methods. *South Afr. J. Bot.* 126, 328–339.
- Yelani, T., Meyer, J.J.M., 2009. Isolation and Identification of Poisonous Triterpenoids from *Elaeodendron Croceum*. Department of Botany, Faculty of Natural and Agricultural Sciences. University of Pretoria. Philosophiae Doctorae Thesis.
- Younus, I., Siddiq, A., Assad, T., Badar, S., Jameel, S., Ashraf, M., 2015. Screening antiviral activity of *Moringa oleifera* L. leaves against foot and mouth disease virus. *Global Vet.* 15 (4), 409–413.